

# Effect of Copper Oxide Nanoparticles as a barrier for Efficiency Improvement in ZnO Dye-Sensitized Solar Cells

A Sonthila, P Ruankham, S Choopun, D Wongratanaphisan,  
S Phadungdhithhada and A Gardchareon\*

Department of Physics and Materials Science, Faculty of Science, Chiang Mai University

salee.gard@gmail.com

**Abstract.** CuO nanoparticles (CuO NPs) were used as a barrier layer in ZnO dye-sensitized solar cells (DSSCs) to obtain high power conversion efficiency. The barrier layer was investigated in terms of the size of CuO NPs by varying power of pulsed Nd:YAG (1064 nm) laser ablation. Morphological and optical properties of CuO NPs were characterized by transmission electron microscopy (TEM), UV-visible spectrophotometry (UV-vis) and dynamic light scattering (DLS). It was found that the CuO NPs are rather spherical in shape with diameter in between 20 - 132 nm. In addition, the energy gap of CuO decreases with the increase of CuO NPs size. The power conversion efficiency of ZnO DSSCs was measured under illumination of simulated sunlight obtained from a solar simulator with the radiant power of 100 mW/cm<sup>2</sup>. The results showed that the ZnO DSSC with the CuO NPs with size of 37 nm exhibits the optimum power conversion efficiency of 1.01% which is higher than that of one without CuO NPs. Moreover, the power conversion efficiency of the ZnO DSSCs decreases with the increase of CuO NPs size.

## 1. Introduction

The initial work on dye-sensitized solar cell (DSSCs) was done by O'Regan and Grätzel in 1991 [1]. Following this idea, the highest efficiency of 11.1% was obtained on DSSCs with mesoporous titanium dioxide (TiO<sub>2</sub>) as semiconductor [2]. Recently, the investigation of ZnO as an alternative photo electrode has been intensively carried out due to the band gap, electron affinity, and electron injection efficiency which are nearly the same as TiO<sub>2</sub>. However, a further increase in power conversion efficiencies of DSSCs has been limited by energy loss due to recombination between the injected electrons and either the oxidized dye molecules or electron-accepting species in the electrolyte during the charge transport process [3-5]. The investigation in order to suppress this process has been intensively carried out [3-8].

In this work, the different sizes of CuO NPs have prepared by laser ablation method then used the nanoparticles as a layer on the top of ZnO layer to form blocking layer in order to control charge recombination dynamics in ZnO DSSCs. The CuO NPs characteristics and the effect of CuO NPs size on photocurrent, photovoltage and power conversion efficiency characteristics for ZnO DSSCs have been investigated.

## 2. Materials and Methods

### 2.1. Preparation and Characterization of CuO nanoparticles

CuO NPs used in this work were fabricated by focusing a radiation from pulsed Nd:YAG laser ablation, operating at the fundamental wavelength of 1064 nm ( Kevron Marker Laser ), on the surface of copper target. The target was 0.3 mm in thickness and the size of  $20 \times 20 \times 0.3 \text{ mm}^3$ . The target was sonicated in acetone and ethanol in an ultrasonic cleaner to remove any organic impurities on its surface for 30 min each before ablation. The cleaned target was immersed in  $7 \text{ cm}^3$  of distilled water and irradiated by laser at different power from 60 to 100 W with pulse frequency of 30,000 Hz for 10 min. Note that the target was kept under the surface of distilled water. The laser ablation was accompanied by the presence of a small plasma plume above the target surface. The aqueous solution light-green color was observed after a few minutes during the ablation, indicating the presence of CuO NPs. The colloidal NPs were investigated by dynamic light scattering (DLS) for particle size analysis, transmission electron microscopy (TEM, JEOL JEM-2010 operating at 200 kV) for the morphology, PDA UV-VIS spectrophotometer (S-2100 Series, SCINCO) for optical transmission spectra. For recording PL spectrum of the colloidal NPs, 632.5 nm line of He-Ne laser was used as excitation source.

### 2.2. Fabrication and Characterization of ZnO Dye-Sensitized Solar Cells.

The DSSCs structures used in this experiment were shown as schematic diagram in Figure 1.

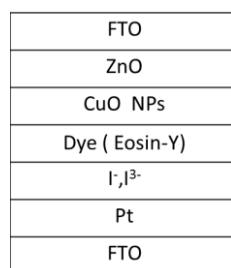


Figure. 1 Schematic diagram of DSSCs structures used in this experiment.

For the ZnO/CuO photoelectrode, ZnO powder paste was prepared by dissolving ZnO powder (99.9% size  $< 1 \mu\text{m}$ , Aldrich) in polyethyleneglycol (PEG 6 %) solution at ratio of ZnO:PEG 1 g : 2  $\text{cm}^2$  by weight. The mixture was stirred for 1 hr before use. ZnO powder paste was screened on FTO glass and heated at  $400 \text{ }^\circ\text{C}$  for 1 h under normal atmosphere to remove PEG. The process was followed by dropping 100  $\mu\text{l}$  of the colloidal CuO NPs on ZnO layer. Then, the photoelectrodes were soaked in Eosin-Y ( $\text{C}_{20}\text{H}_6\text{Br}_4\text{Na}_2\text{O}_5$ ) organic dye solution ( $5.8 \times 10^{-4} \text{ mol/l}$   $\text{C}_{20}\text{H}_6\text{Br}_4\text{Na}_2\text{O}_5$ , in ethanol) for 1 h. For the counter-electrode,  $\text{Cl}_6\text{H}_2\text{Pt.aq}$  (20 mM hydrogen hexachloroplatinate (IV) hydrate in acetone solution) was dropped on FTO glass and heated at  $550 \text{ }^\circ\text{C}$  for 1 hr. The photoelectrode and the counterelectrode were compiled into a sealed device using a hot-melted double layer parafilm and the redox electrolyte (0.03 M  $\text{I}_2$ + 0.3 M LiI in polyethylene carbonate solution) was introduced into the inter-space between the photoelectrode and the counter-electrode through two predrilled holes on the side of the device.

The photocurrent, photovoltage and power conversion efficiency characteristics for ZnO DSSCs were measured under illumination of simulated sunlight coming from a solar simulator with the radiant power of  $100 \text{ mW/cm}^2$  from xenon lamp with AM 1.5 filter (Solar Light CO. model XPS 400). The photocurrent densities versus photovoltage ( $J$ - $V$ ) characteristics were measured with dc voltage and current source which were interfaced and controlled by computer. The open circuit voltage ( $V_{\text{OC}}$ ), the short current density ( $J_{\text{SC}}$ ), fill factor ( $FF$ ) and overall power conversion efficiency ( $\eta$ ) were extracted from the  $J$ - $V$  curve.

### 3. Results and discussion

#### 3.1. Characteristics of CuO NPs

The TEM images in Figure 2(a), 2(b), 2(c), 2(d) and 2(e) of the products prepared at the different power of 60, 70, 80, 90 and 100 W, respectively, show that their consist of rather spherical particles. The selected area electron diffraction patterns ( SADPs ) in Figure 2(f), 2(g), 2(h), 2(i) and 2(j) show the concentric electron diffraction rings correspond to (002), (111), (112) and (202) planes which indicates the CuO structure according to the diffraction pattern of CuO from JCPDS No. 80-1917.

Size distributions of the CuO NPs prepared at different power were measured from dynamic light scattering (DLS). It was found that the CuO NPs size was increased with the increasing of laser power. The mean size of CuO NPs were 20, 28, 32, 79 and 132 nm for CuO NPs prepared at (a) 60 W, (b) 70 W, (c) 80 W, (d) 90 W and (e) 100 W, respectively.

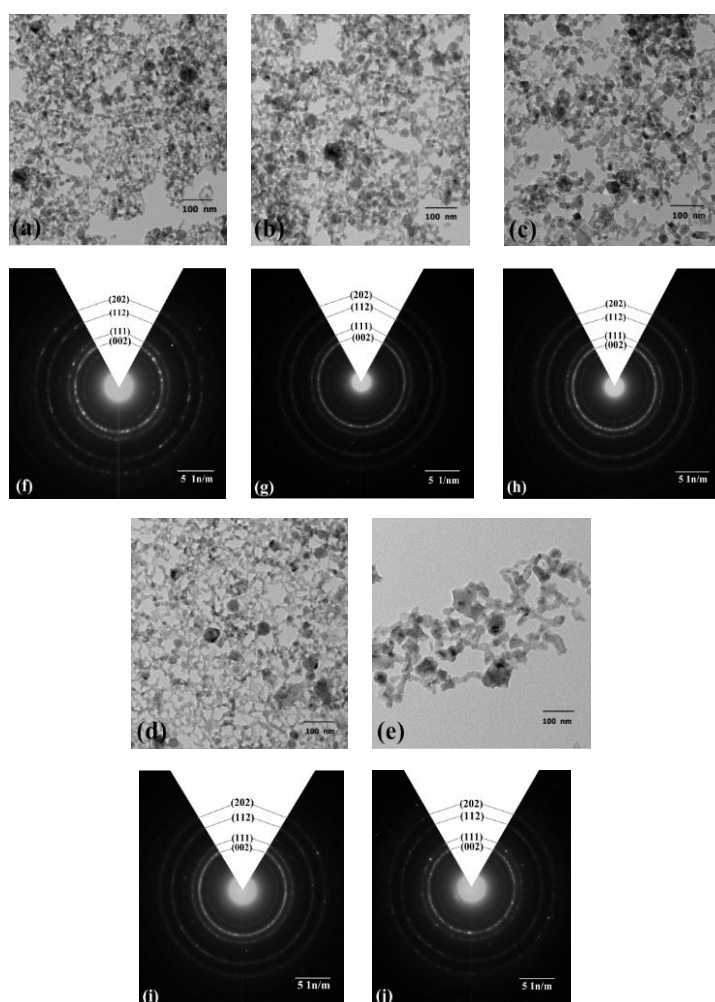


Figure. 2 TEM image of the product prepared at at different power (a) 60 W, (b) 70 W, (c) 80 W, (d) 90 W and (e) 100 W with corresponding to electron diffraction pattern in (f), (g), (h), (i) and (j), respectively.

### 3.2. Optical properties

The transmittance spectrum of the colloidal CuO NPs prepared at various power conditions were shown in Figure 3. The energy band gap of the colloidal CuO NPs can be extracted from transmittance spectra. An estimated optical band gap is obtained using the following equation [9]:

$$\alpha hv = (hv - E_g)^n ; \quad \alpha = 2.3026 \frac{A}{t}$$

where  $A$  is constant called absorption coefficient,  $t$  is the film thickness,  $h\nu$  is the photon energy,  $E_g$  is band gap. The value of  $n$  depends on the nature of transition. Depending on whether the transition is direct transition, direct forbidden, or indirect transition,  $n$  takes the value  $1/2$ ,  $3/2$  or  $2$  respectively [10]. The value of the band gap is obtained by plotting the graph between  $(\alpha hv)^{1/2}$  versus photon energy ( $h\nu$ ) gives the value of indirect band gap. The extrapolation of the linear portion of the curve to  $(\alpha hv)^{1/2} = 0$ , gives the value of band gap as shown in the inset of Figure 3.

It is observed from the inset of Figure 3 that the energy gap of the colloidal CuO NPs prepared at power of 60 - 100 W were in a range of 2.01 - 2.42 eV. This value is larger than that of the reported value for bulk CuO ( $E_g = 1.2$  eV) [11]. Therefore, the difference in the band gap of nanoparticles is indicative of variance size. For small particles, quantum confinement effect occurs with potential wells of small lateral dimension and the energy difference between the position of the conduction band and a free electron, which leads to a quantization of their energy levels. The increase in the band gap of the as-prepared CuO nanoparticles is indicative of quantum size effect [12].

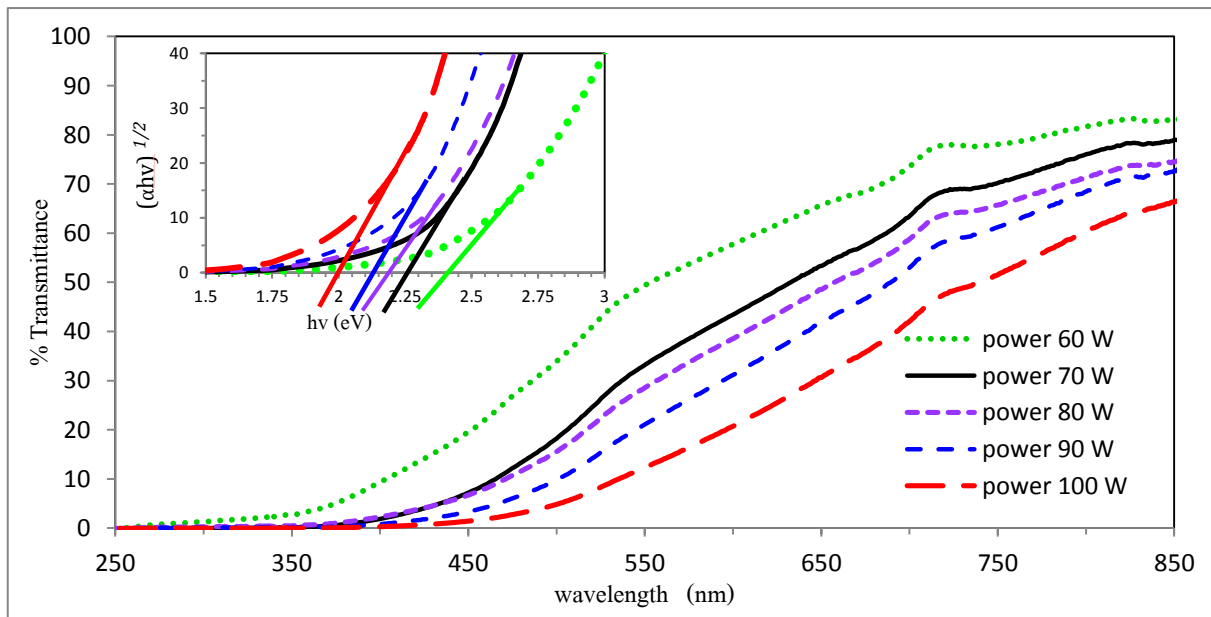


Figure. 3 Transmission spectrum of the colloidal CuO NPs prepared at various power conditions

### 3.3. $J$ - $V$ Characteristics of DSSCs

Figure 4 showed  $J$ - $V$  characteristics of ZnO DSSCs with ZnO/CuO NPs with different size layer as a photo-electrode. For comparison,  $J$ - $V$  characteristics of ZnO DSSCs without CuO NPs was also shown in Figure 4. The important parameters such as short circuit current density ( $J_{sc}$ ), open circuit voltage ( $V_{oc}$ ), fill factor ( $FF$ ) and power conversion efficiency ( $\eta$ ) which determined from the measured  $J$ - $V$  curves were summarized in Table 1.

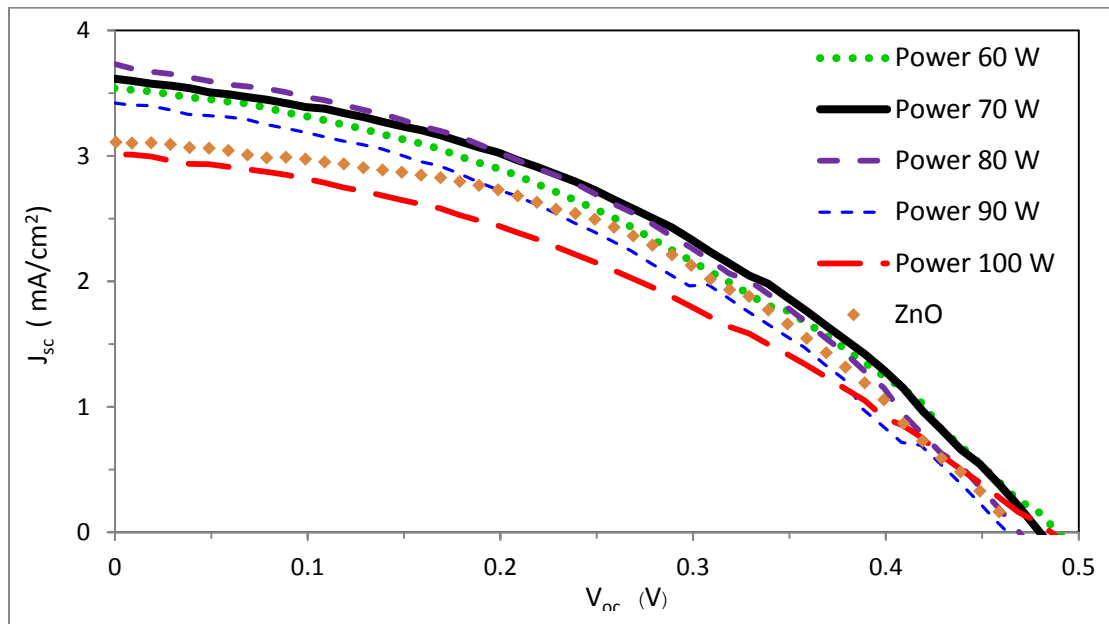


Figure. 4  $J$ - $V$  characteristic of ZnO, ZnO/CuO NPs (prepared at various power conditions) layer as photo-electrode of the DSSCs .

Table 1. Comparison of DSSCs parameters such as short circuit current density ( $J_{sc}$ ), open circuit voltage ( $V_{oc}$ ), fill factor ( $FF$ ) and power conversion efficiency ( $\eta$ ).

Power (Watt)	Size particles (nm)	$V_{oc}$ (Volt)	$J_{sc}$ ( $\text{mA}/\text{cm}^2$ )	FF	$\eta$ (%)
ZnO	-	0.46	3.11	0.45	0.65
60	20	0.49	3.53	0.38	0.82
70	28	0.48	3.61	0.41	0.94
80	32	0.47	3.73	0.40	1.01
90	79	0.46	3.42	0.39	0.71
100	132	0.46	3.04	0.38	0.54

It was clearly seen that the power conversion efficiency value of ZnO DSSCs with CuO NPs as a barrier layer depend on CuO NPs size. The power conversion efficiency increases with the increase of CuO NPs size. The value reaches the maximum at CuO NPs size of 32 nm, then it decreases with the larger CuO NPs size. The highest short current density of  $3.73 \text{ mA}/\text{cm}^2$  and the highest power

conversion efficiency of  $\eta = 1.01\%$  was obtained from DSSCs with CuO NPs size of 32 nm, prepared at 80 W of laser power. This result corresponds to the work of Thanoi et. al. [8]. Beside that the power conversion efficiency of the ZnO DSSCs with CuO NPs in this work is higher than ZnO DSSCs with CuO thin film, CuO power and CuO nanowires which reported by Raksa et al [7]. This is due to the energy gap of CuO NPs is higher than the others then it can suppress more back electron transfer in recombination process. The ZnO DSSCs with the CuO NPs exhibited higher power conversion efficiency than that without CuO NPs indicates that the improvement of the efficiency could be explained in terms of CuO barrier layer as a potential step in energy band diagram since CuO has higher conduction band level than ZnO but lower than the LUMO level of Eosin-Y dye [7].

#### 4. Conclusions

We have successfully synthesized different size of CuO NPs by varying the power of Nd:YAG pulsed laser ablation. The CuO NPs were found to be rather spherical shape with diameter in between 20 - 132 nm and the energy gap are approximately about 2.01 -2.42 eV. The obtained CuO NPs with different size were used as a barrier layer for efficiency improvement of ZnO DSSCs. It was found that the power conversion efficiency of ZnO DSSCs with the CuO NPs depends on the CuO NPs size. The ZnO DSSCs with the CuO NPs exhibited the optimum power conversion efficiency of 1.03%. The ZnO DSSCs with the CuO NPs exhibited higher power conversion efficiency than that without CuO NPs. This could be explained in terms of suppression of back electron transfer in recombination process.

#### Acknowledgements

We are grateful to the Ministry of Science and Technology of Thailand for financial support. Anongnart Sonthila would like to acknowledge the Graduate School, Chiang Mai University.

#### References

- [1] O'Regan B. and Grätzel M. 1991 "A lowcost, high-efficiency solar cell based on dye-sensitized colloidal TiO<sub>2</sub> films", *Nature* p737-740.
- [2] Y. Chiba, A. Islam, Y. Watanabe, R. Komiya, N. Koide and L. Han 2006 "Dye-sensitized solar cells with conversion efficiency of 11.1%" *Jpn. J. Appl. Phys.* p638.
- [3] J. Nissfolk, K. Fredin, A. Hagfeldt, G. Boschloo, 2006 *J. Phys. Chem. B* p 110.
- [4] M. Gratzel, *Inorg. Chem.* 2005, 44, 6841.
- [5] M. Gratzel 2004 *J. Photochem. Photobiol. A* p164.
- [6] J. Bandara, U.W. Pradeep, R.G.S.J. Bandara 2005 "The role off n-p junction electrodes in minimizing the charge recombination and enhancement of photocurrent and photovoltage in dye sensitized solar cells". *Photochem. Photobiol., A. Chem.* p 273.
- [7] P. Raksa, S. Nilphai, A. Gardchareon, and S. Choopun 2009 "Copper oxide thin film and nanowire as a barrier in ZnO dyn-sensitized solar cells" *Thin solid Films* p 4741.
- [8] D.Thanoi, D. Wongratanaphisan, S.Choopun, and A.Gardchareon 2012 "Copper Oxide Nanoparticles as a barrier in ZnO Dye-Sensitized Solar Cells" (Proceeding of Siam Physics Congress,Thailand, May)
- [9] N.F. Mott, E.A. Davies,1979 "Electronic Processes in Non-Crystalline Materials ",(Clarendon Press, Oxford).
- [10] A.N. Banerjee and K.K. Chattopadhyay, in D. Depla and S. Maheiu (Eds.),2008 "Reactive Sputter Deposition", *Springer-Verlag Berlin Heidelberg* p.465.
- [11] Wasil Abdalgader Abdalla Alhassan etal. 2014 "Determination of energy gap copper oxide by four probe methods", *Intern.J.Ren.Ener.Technol.Res* p1-8.
- [12] J.P. Yang, F.C. Meldrum, J.H. Fendler,1995 *J. Phys. Chem.* p 5500.